Chemistry & Biology
Article

Development of Pyrrole-Imidazole Polyamide for Specific Regulation of Human Aurora Kinase-A and -B Gene Expression

Teruyuki Takahashi,[1,2,*] Yukihiro Asami,[2] Eiko Kitamura,[1] Tsukasa Suzuki,[2] Xiaofei Wang,[2] Jun Igarashi,[1] Aiko Morohashi,[1] Yui Shinojima,[2] Hisao Kanou,[2] Kosuke Saito,[1] Toshiaki Takasu,[1] Hiroki Nagase,[1,2] Yuichi Harada,[3] Kazumichi Kuroda,[3] Takayoshi Watanabe,[4] Satoshi Kumamoto,[4] Takahiko Aoyama,[5] Yoshiaki Matsumoto,[5] Toshikazu Bando,[6] Hiroshi Sugiyama,[6] Chikako Yoshida-Noro,[1] Noboru Fukuda,[1] and Nariyuki Hayashi[1]
[1]Advanced Research Institute for the Sciences and Humanities, Nihon University, Tokyo, Japan
[2]Division of Cancer Genetics, Department of Advanced Medical Science
[3]Division of Microbiology, Department of Pathology and Microbiology
Nihon University School of Medicine, Tokyo, Japan
[4]Gentier Biosystems Incorporation, Kyoto, Japan
[5]Department of Clinical Pharmacokinetics, College of Pharmacy, Nihon University, Chiba, Japan
[6]Department of Chemistry, Graduate School of Science, Kyoto University, Kyoto, Japan
*Correspondence: teruyuk@med.nihon-u.ac.jp
DOI 10.1016/j.chembiol.2008.06.006

SUMMARY

Pyrrole-imidazole polyamide (PIP) is a nuclease-resistant novel compound that inhibits gene expression through binding to the minor groove of DNA. Human aurora kinase-A (AURKA) and -B (AURKB) are important regulators in mitosis during the cell cycle. In this study, two specific PIPs (PIP-A and PIP-B) targeting AURKA and AURKB promoter regions were designed and synthesized, and their biological effects were investigated by several in vitro assays. PIP-A and PIP-B significantly inhibited the promoter activities, mRNA expression, and protein levels of AURKA and AURKB, respectively, in a concentration-dependent manner. Moreover, 1:1 combination treatment with both PIPs demonstrated prominent antiproliferative synergy (CI value [ED_{50}] = 0.256) to HeLa cells as a result of inducing apoptosis-mediated severe catastrophe of cell-cycle progression. The novel synthesized PIP-A and PIP-B are potent and specific gene-silencing agents for AURKA and AURKB.

INTRODUCTION

Small molecules that preferentially bind to predetermined DNA sequences inside living cells would be useful tools in molecular biology and, perhaps, in human medicine (Bando et al., 2002; Best et al., 2003; Bischoff et al., 1998; Carvajal et al., 2006; Chou and Talalay, 1984). The effectiveness of these small molecules requires not only that they bind to chromosomal DNA in a site-specific manner, but also that they are permeable to the outer membrane and gain access to the nuclei of living cells (Best et al., 2003; Dervan, 2001; Nickols and Dervan, 2007; Nickols et al., 2007; Trauger et al., 1996).

Pyrrole-imidazole polyamide (PIP) was first identified from ducarmycin A and distamycin A by Dervan, et al. (Best et al., 2003; Dervan, 2001; Nickols and Dervan, 2007; Nickols et al., 2007; Trauger et al., 1996). PIPs are small synthetic molecules composed of the aromatic amino acids *N*-methylpyrrole (Py) and *N*-methylimidazole (Im) (Bando et al., 2002; Best et al., 2003; Dervan, 2001; Matsuda et al., 2006; Murty and Sugiyama, 2004; Nickols and Dervan, 2007; Nickols et al., 2007; Trauger et al., 1996; Zhang et al., 2006). Synthetic PIPs recognize and bind to specific nucleotide sequences in the minor groove of double-helical DNA with high affinity and block the binding of specific proteins (Bando et al., 2002; Best et al., 2003; Dervan, 2001; Matsuda et al., 2006; Murty and Sugiyama, 2004; Nickols and Dervan, 2007; Nickols et al., 2007; Trauger et al., 1996; Zhang et al., 2006). There is a set of pairing rules for the interaction between these heterocyclic rings (Py and Im) and nucleotide base pairs in the minor groove; pairing of Im opposite Py (Im/Py) specifically binds to the G-C base pair, Py/Im is specific for the C-G base pair, and Py/Py binds to both the A-T and T-A base pairs (Bando et al., 2002; Best et al., 2003; Dervan, 2001; Matsuda et al., 2006; Murty and Sugiyama, 2004; Nickols and Dervan, 2007; Nickols et al., 2007; Trauger et al., 1996; Zhang et al., 2006). In addition, synthetic PIPs are resistant to nucleases and do not require particular delivery systems, unlike such conventional gene silencing agents as antisense DNA, ribozymes, and siRNA (Bando et al., 2002; Best et al., 2003; Dervan, 2001; Matsuda et al., 2006; Murty and Sugiyama, 2004; Nickols and Dervan, 2007; Nickols et al., 2007; Trauger et al., 1996; Zhang et al., 2006). Therefore, PIPs may be useful tools in molecular biology medicine.

Members of the Aurora/Ipl1p kinase family, which are among the serine/threonine kinases, are highly conserved in diverse eukaryotes and are thought to play important roles in normal chromosome segregation and cytokinesis (Carvajal et al., 2006; Kimura et al., 2004; Tanaka et al., 2002). Three types of human Aurora/Ipl1p family protein kinases—Aurora kinase-A (AURKA), Aurora kinase-B (AURKB), and Aurora kinase-C (AURKC) —have been identified in different aspects of mitosis (Carvajal et al., 2006; Kimura et al., 2004; Tanaka et al., 2002). AURKA localizes to centrosomes and is required for centrosome

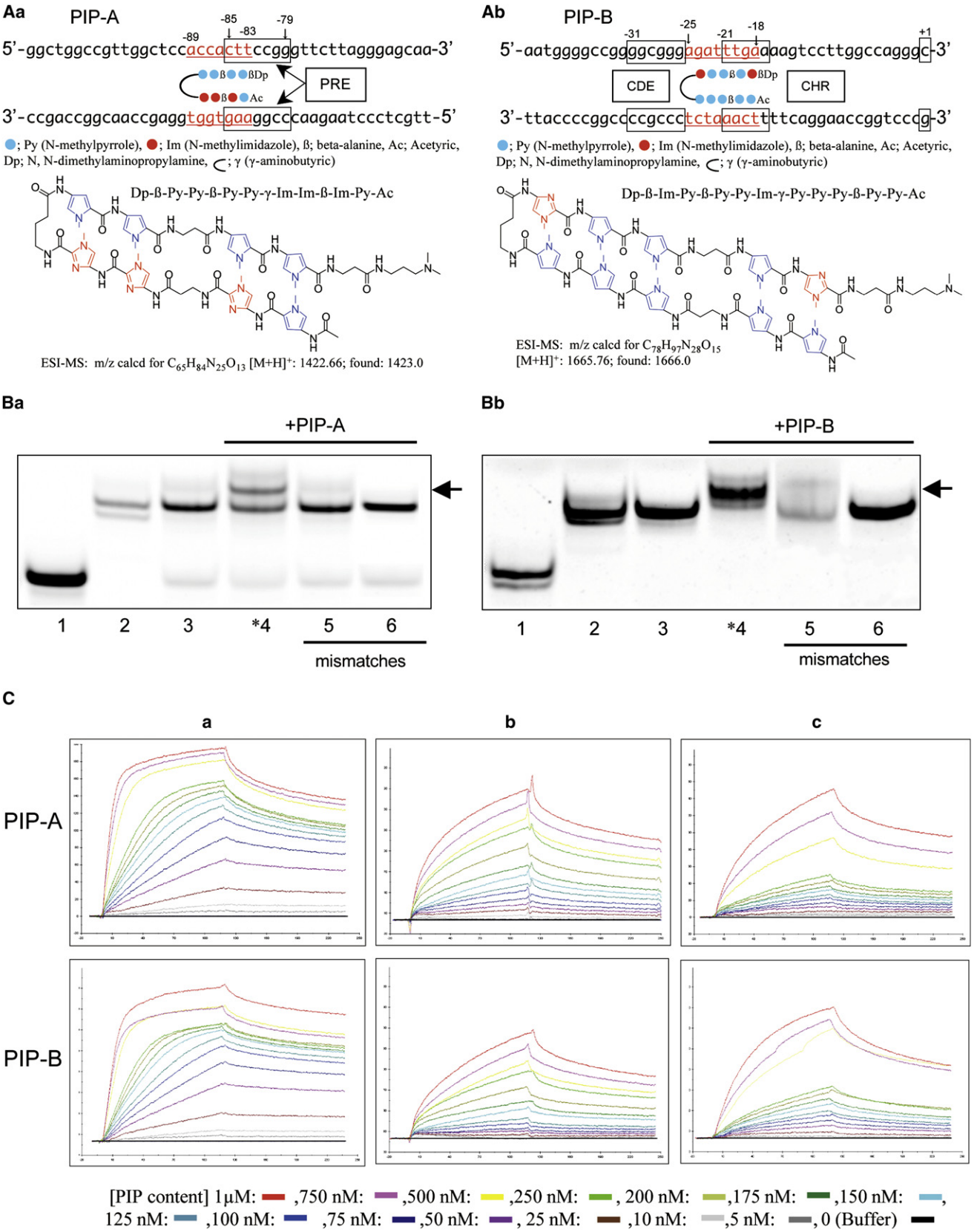
Aa
PIP-A
5'-ggctggccgttggctccaccacttccgggttcttagggagcaa-3'
PRE
3'-ccgaccggcaaccgaggtggtgaaggcccaagaatccctcgtt-5'
●; Py (N-methylpyrrole), ●; Im (N-methylimidazole), ß; beta-alanine, Ac; Acetyric, Dp; N, N-dimethylaminopropylamine, ⊂; γ (γ-aminobutyric)
Dp-ß-Py-Py-ß-Py-Py-γ-Im-Im-ß-Im-Py-Ac
ESI-MS: m/z calcd for C65H84N25O13 [M+H]+: 1422.66; found: 1423.0
Ab
PIP-B
5'-aatggggccgggcgggagaatttgaaaagtccttggccagggc-3'
CDE
CHR
3'-ttaccccggccccgcccctctaaacttttcaggaaccggtcccg-3'
●; Py (N-methylpyrrole), ●; Im (N-methylimidazole), ß; beta-alanine, Ac; Acetyric, Dp; N, N-dimethylaminopropylamine, ⊂; γ (γ-aminobutyric)
Dp-ß-Im-Py-ß-Py-Py-Im-γ-Py-Py-Py-ß-Py-Py-Ac
ESI-MS: m/z calcd for C78H97N28O15 [M+H]+: 1665.76; found: 1666.0
Ba
+PIP-A
1 2 3 *4 5 6
mismatches
Bb
+PIP-B
1 2 3 *4 5 6
mismatches
C
a
b
c
PIP-A
PIP-B
[PIP content] 1μM: ,750 nM: ,500 nM: ,250 nM: , 200 nM: ,175 nM: ,150 nM: , 125 nM: ,100 nM: ,75 nM: ,50 nM: , 25 nM: ,10 nM: ,5 nM: , 0 (Buffer)

maturation, spindle formation, and extension of microtubules (Carvajal et al., 2006; Tanaka et al., 2002). AURKB demonstrates a typical localization pattern of chromosomal passenger proteins that relocate from the centromeres to the equatorial region along the midzone after the onset of anaphase (Carvajal et al., 2006; Kimura et al., 2004). AURKB is an essential factor for chromosome alignment, kinetochore-microtubule attachment, chromosome segregation, and cytokinesis (Carvajal et al., 2006; Kimura et al., 2004). AURKC is specifically and abundantly expressed in the testis, where it functions in spermatogenesis and regulation of cilia and flagella. However, its role in cancer development is currently unclear (Carvajal et al., 2006). AURKA and AURKB mRNA expressions are regulated in a cell-cycle-dependent manner (Carvajal et al., 2006; Kimura et al., 2004; Tanaka et al., 2002). The levels of mRNA, protein, and kinase activity in both AURKA and AURKB are low during the G1/S phase, accumulate during the G2/M phase, and decrease rapidly after mitosis (Carvajal et al., 2006; Kimura et al., 2004; Tanaka et al., 2002). Their ectopic overexpression in cultured cells leads to centrosome abnormality and chromosome aneuploidy, and then results in either cell death or survival through malignant transformation (Bischoff et al., 1998; Carvajal et al., 2006; Jung et al., 2006; Kanda et al., 2005; Kimura et al., 2004; Meraldi et al., 2002; Ota et al., 2002; Sorrentino et al., 2005; Tanaka et al., 2002). In addition, the high-level expression of AURKA or AURKB is exhibited in various human cancer cells and tumor cell lines (Bischoff et al., 1998; Carvajal et al., 2006; Jung et al., 2006; Kanda et al., 2005; Kimura et al., 2004; Meraldi et al., 2002; Ota et al., 2002; Sorrentino et al., 2005; Tanaka et al., 2002).

To develop novel anticancer agents, the authors designed and synthesized two specific PIPs targeting AURKA and AURKB promoter regions. These synthetic PIPs—PIP-A and PIP-B for AURKA and AURKB promoter, respectively—were investigated, and their biological effects in cellular systems were evaluated by use of in vitro assays.

RESULTS

Structure of Novel PIPs Targeting AURKA and AURKB Promoter

The gene encoding AURKA is located on chromosome 20q13.2 (Carvajal et al., 2006; Tanaka et al., 2002), and the sequence is available from the DDBJ/EMBL/GenBank™ data base (accession number AL121914). The PIP targeting AURKA (PIP-A) was designed to span the boundary of the previously reported positive regulatory element (PRE) (−85 to −79) on the AURKA promoter, and it recognized 7 bp (Figure 1Aa; Tanaka et al., 2002). The gene encoding AURKB is located on chromosome 17p13.1 (accession number AC135178) (Carvajal et al., 2006; Kimura et al., 2004). The PIP targeting AURKB (PIP-B) was designed to span the boundary of the previously reported cell-cycle gene homology region (CHR) (−21 to −17) on the AURKB promoter, and it recognized 8 bp (Figure 1Ab; Kimura et al., 2004). The numberings refer to the previously reported major transcriptional initiation site as +1 (Figure 1A; Kimura et al., 2004; Tanaka et al., 2002). PRE and CHR were previously described as playing important roles in the cell-cycle-dependent regulation of AURKA or AURKB gene expression (Kimura et al., 2004; Tanaka et al., 2002).

The structures of both novel synthesized PIPs (PIP-A and PIP-B) are shown in Figure 1A. The physical and chemical characterizations of both PIPs, as analyzed by electrospray ionization mass spectrometry (ESI-Mass) and HPLC, are shown in Figure S1 available online. The PIPs were dissolved in DMSO at 10 mM, were stored at room temperature, and then were freshly diluted to appropriate concentrations in pure water or growth medium.

DNA-Binding Assay Results

Electromobility shift assay (EMSA) and Biacore assays allow for determination of the binding affinity and specificity of PIP-A and PIP-B for target nucleotide sequences. In EMSA, PIP-A bound to the appropriate 22 bp AURKA "match" double strand (ds)-oligonucleotides (oligo) (Table S1). The clear mobility band that indicates specific binding of PIP-A and match ds-oligo was demonstrated in Figure 1Ba, lane 4, whereas PIP-A did not bind to the 2 bp mutated "mismatch-1" ds-oligo and "mismatch-2" alternate AURKB ds-oligo (Table S1). No mobility band was detected for both mismatch ds-oligos (Figure 1Ba, lanes 5 and 6). Similarly, PIP-B also bound to the appropriate 22 bp AURKB match ds-oligo but did not bind to both mismatch-1 and mismatch-2 ds-oligos (Table S1; Figure 1Bb, lanes 4, 5, and 6).

The kinetics of interaction between PIP and match or mismatch ds-oligo was measured by Biacore assay (Table S1). In surface plasmon resonance sensorgrams, fast and strong bindings of PIP-A and PIP-B to the appropriate AURKA and AURKB match ds-oligo were demonstrated, and these match bindings reached equilibrium at high PIP concentrations (Figure 1Ca), whereas the bindings between both PIPs and the 2 bp mutated mismatch-1 ds-oligo or mismatch-2 alternate AURKB or AURKA ds-oligo were weak and easily dissociated (Figure 1Cb and 1Cc). The kinetic constants calculated from fitting resulting sensorgrams are described in Table 1. Association equilibrium constants (K_A) for the interaction between both PIPs and match

Figure 1. DNA-Binding Assay Results

(A) Target sequence and structure of PIP-A (Aa) and PIP-B (Ab) targeting AURKA or AURKB promoter.

(B) Electromobility shift assay (EMSA) results.

(Ba) PIP-A bindings for oligonucleotides (oligo). Lane 1, ss-oligo; lane 2, match ds-oligo; lane 3, mismatch-1 ds-oligo (equivalent to 2 base mutation oligo-DNA); *lane 4, PIP-A with match ds-oligo; lane 5, PIP-A with mismatch-1 ds-oligo; lane 6, PIP-A with mismatch-2 ds-oligo (alternative use).

(Bb) PIP-B bindings for oligonucleotides (oligo). Lane 1, ss-oligo; lane 2, match ds-oligo; lane 3, mismatch-1 ds-oligo; *lane 4, PIP-B with match ds-oligo; lane 5, PIP-B with mismatch-1 ds-oligo; lane 6, PIP-B with mismatch-2 ds-oligo (alternative use). The clear mobility band that indicates specific binding of PIP-A and PIP-B for each match ds-oligo was demonstrated in *lane-4, whereas no mobility band was detected for mismatch ds-oligos (lanes 5 and 6).

(C) Biacore assay results. Typical surface plasmon resonance sensorgrams for the interactions between respective PIP and match or mismatch ds-oligo are demonstrated.

(Ca) PIP and match ds-oligo interaction. (Cb) PIP and mismatch-1 (equivalent to 2 base mutation) ds-oligo interaction. (Cc) PIP and mismatch-2 (alternatively use) ds-oligo interactions.

Table 1. Kinetic Constants for Binding Between PIP and Match or Mismatch Oligo

PIP	Target/Type	K_a (1/Ms)	K_d (1/s)	K_A (1/M)	K_D (M)	χ^2
PIP-A	match oligo: AURKA	3.84E+05	5.11E-04	7.51E+08	1.33E-09	1.04
	mismatch-1 oligo:2 base mutation AURKA	4.42E+03	3.17E-03	1.39E+06	7.17E-07	0.91
	mismatch-2 oligo:AURKB (alternately use)	1.72E+03	3.59E-03	4.79E+05	2.09E-06	1.31
PIP-B	match oligo: AURKA	5.47E+05	2.68E-04	2.04E+09	4.90E-10	1.36
	mismatch-1 oligo:2 base mutation AURKA	5.41E+03	2.19E-03	2.47E+06	4.05E-07	1.37
	mismatch-2 oligo:AURKB (alternately use)	3.40E+03	4.64E-03	7.33E+05	1.36E-06	0.93
	Specificity					
	match/mismatch-1	match/mismatch-2				
PIP-A	539	1568				
PIP-B	826	2785				

The kinetic constants were calculated from the surface plasmon resonance sensorgrams for the interaction between PIP compounds and biotin labeled match or mismatch oligo-DNA that were immobilized respectively on a sensor chip SA (Biacore assays). Specificity was defined as K_A (match binding)/K_A (mismatch binding).
K_a, association rate constant; K_d, dissociation rate constant; K_A, association equilibrium constant; K_D, dissociation equilibrium constant.

ds-oligo demonstrated higher values than those for the interaction between both PIPs and two types of mismatch ds-oligo. The specificity for binding of PIP to target nucleotide sequences was defined as K_A (match binding)/K_A (mismatch binding) (Table 1). These data indicated that both PIP-A and PIP-B specifically and independently bound to the respective target nucleotide sequence.

Distribution of FITC-Labeled PIP In Vitro

The distributions of FITC-labeled PIP-A and PIP-B in HeLa cells after 6 and 12 hr incubation are shown in Figure 2. Both FITC-labeled PIPs in growth medium immediately permeated into cytoplasm from outer membrane,and localized in all nuclei of HeLa cells incubated for 6 hr. In HeLa cells incubated for 12 hr, the prominent accumulation and condensation of both FITC-labeled PIPs in nuclei was demonstrated. In addition, both FITC-labeled PIPs were present in all nuclei by 24 and 48 hr (data not shown).

Induction of AURKA and AURKB mRNA Expression and Knockdown Effects of PIP-A and PIP-B During G2/M Phase

HeLa cells were synchronized at the G1/S boundary by use of the double thymidine block (DTB) protocol, as described elsewhere (Tanaka et al., 2002), followed by release. Laser-scanning

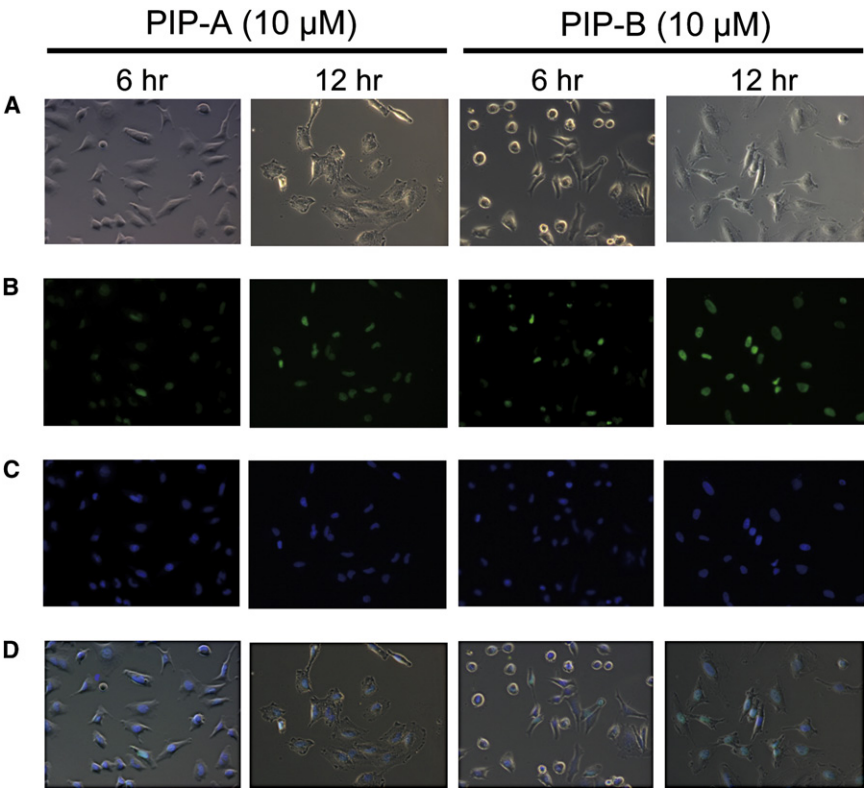

Figure 2. Celluar Localization of FITC-Labeled PIP
The distributions of FITC-labeled PIP-A and PIP-B in HeLa cells after 6 and 12 hr of incubation are demonstrated.
(A) Bright field.
(B) FITC.
(C) Hoechst 33342.
(D) Merge.

cytometry (iCys System™; CompuCyte Corp.) confirmed that more than 75% of the cells were arrested in the G1 phase at "time 0" (Figure 4A). After release from DTB, the cells were predominantly (more than 70%) in the G2/M phase at 10 hr (Figures 3A and 3B).

The induction of AURKA and AURKB mRNA expression during the G2/M phase was confirmed through real-time quantitative PCR assay by using synchronized HeLa cell populations. The levels of both AURKA and AURKB mRNA expressions were about three times higher in the G2/M phase than in the G1 phase (Figures 3C and 3D), which is consistent with the results of previous investigations (Kimura et al., 2004; Tanaka et al., 2002). In addition, the knockdown effects of PIP-A and PIP-B for AURKA and AURKB mRNA expression during the G2/M phase were identified by real-time quantitative PCR assay. Both PIP-A and PIP-B (10 μM each) demonstrated significant knockdown effects (**$p < 0.01$; asterisks denote a statistically significant difference) for mRNA expression of AURKA (knockdown-efficiency [KDE] = 55.9%) and AURKB (KDE = 64.2%) in the G2/M phase (Figures 3C and 3D). Mismatch PIP (10 μM each of alternate PIP-B or PIP-A) did not affect respective mRNA expression.

Knockdown Effect of PIP-A and PIP-B for Promoter Activities, mRNA Expression, and Protein Levels of AURKA and AURKB in Random Cultured Cells

In random cultured cell populations, both luciferase activity in HeLa cells that were transfected with AURKA and AURKB promoter plasmids (Figure S2) and mRNA expression of AURKA (Figure 3E) and AURKB (Figure 3F) peaked during 12 hr of incubation, which is almost consistent with cell-cycle synchronization analysis results. Both PIP-A and PIP-B significantly decreased (**$p < 0.01$) luciferase activity (Figure S2) and mRNA expression of AURKA and AURKB (Figures 3E and 3F) during 12 hr of incubation in a concentration-dependent manner. In random cultured cell populations, 10 μM of both PIP-A and PIP-B demonstrated knockdown effects for mRNA expression of AURKA (KDE = 53.5%) and AURKB (KDE = 51.2%) that were almost equivalent to those in synchronized cell populations. In addition, the 1:1 combination treatment with PIP-A and PIP-B (5 μM each) demonstrated significant knockdown effects (**$p < 0.01$) for respective mRNA expression.

The protein levels of AURKA and AURKB were confirmed by Western blot (WB) analysis (Figure 3G). In 12 hr random cultured HeLa cells, treatment of cells with PIP-A and PIP-B demonstrated a prominent reduction of the respective AURKA and AURKB protein levels in a concentration-dependent manner, compared with that in nontreated control cells (including 1% DMSO). The knockdown effects of both PIPs, in particular 10 μM, for protein levels were almost consistent with those for mRNA expression. In addition, the 1:1 combination treatment with PIP-A and PIP-B (5 μM each) also demonstrated sufficient reduction for the respective AURKA and AURKB protein levels. Actin-β used as a loading control demonstrated steady-state levels in all WB analysis. As supporting reference experiments, HeLa cells were transfected with siRNA to repress AURKA or AURKB, respectively (siRNA-A and siRNA-B; Table S1). The siRNA-A or siRNA-B repressed each protein level, similar to the results of both PIPs treatment (Figure 3G).

Mismatch PIP (10 μM of alternate PIP-B or PIP-A) did not affect promoter activity (Figure S2), mRNA expression, or protein levels of AURKA and AURKB (Figures 3E–3G). Moreover, in WB analysis, AURKB blot (mismatch) on extracts treated with PIP-A and AURKA blot (mismatch) on extracts treated with PIP-B revealed steady-state levels (Figure 3G). These results indicated that both PIP-A and PIP-B act as potent and specific inhibitors for mRNA expression of AURKA and AURKB by independently repressing each promoter activity.

In Vitro Cell Viability Assay and Combination Assay Results

The effects of both PIPs against several human tumor cell lines were examined by in vitro cell viability assay under the random cultured cells condition. The effects of both PIPs against HeLa cells were assessed at 48 hr (Figure 4A and Table 2). The PIP-B treatment result demonstrated more significant loss of viability (IC_{50} = 11.76 μM), compared with the PIP-A treatment result (IC_{50} = 25.47 μM). Moreover, the 1:1 combination treatment with PIP-A and PIP-B revealed a potent antiproliferative effect for HeLa cells (IC_{50} = 5.89 μM), compared with treatment with either single PIP. On the basis of the data shown in Figure 4A, the isobologram and combination index (CI) value were calculated by use of the previously established median-effect algorithm (Chou and Talalay, 1984; Damaraju et al., 2007) using CalcuSyn software (version 2.0; Biosoft). The isobologram at 1:1 combination treatment was constructed for effective dose (ED) 50, 75, and 90, indicating 50%, 75%, and 90% growth inhibition, respectively (Figure 4B). The CI value at 1:1 combination treatment was 0.256 (<1.0) (Table 2); therefore, the potent antiproliferative synergy was demonstrated. In addition, the combination assays were performed at different combination ratio of 3:1 or 1:3 (PIP-A:PIP-B). As a result, PIP-B's dominant antiproliferative synergy (CI values = 0.655 and 0.259 for 3:1 and 1:3 combination) was indicated (Table 2).

Two reference experiments were performed. As the first reference experiment, cisplatin was examined as an existent antitumor agent, and its IC_{50} value for HeLa cells was 33.92 μM (Table 2). These data indicate that a specific DNA-binding agent such as PIP might have more potent antiproliferative activity for human tumor cells rather than a nonspecific DNA-binding agent such as cisplatin. As the second reference experiment, the antiproliferative effects of siRNA-A and siRNA-B (Table S1) were also examined with and without the use of lipofection. With lipofection, the single treatment with siRNA-A or siRNA-B demonstrated more-potent antiproliferative effects for HeLa cells, compared with PIP-A or PIP-B (Figure 4C and Table 2). These results reflect the high KDE of both siRNAs and are consistent with WB analysis results (Figure 3G). Moreover, in HeLa cells that were double transfected with siRNA-A and siRNA-B, antiproliferative synergy (CI value = 0.525) was demonstrated, similar to the results of combination treatment with PIP-A and PIP-B (Figure 4C and Table 2). Without lipofection, both siRNAs demonstrated no antiproliferative effect for HeLa cells properly (Figure 4C).

The antiproliferative synergy of the 1:1 combination treatment was examined for other several human tumor cell lines assessed at 48 hr (Figure 4D and Table 2).Overexpression of the AURKA or AURKB genes in these selected human tumor cell lines has already been reported by previous investigators (Bischoff et al., 1998; Carvajal et al., 2006; Kanda et al., 2005; Kimura et al.,

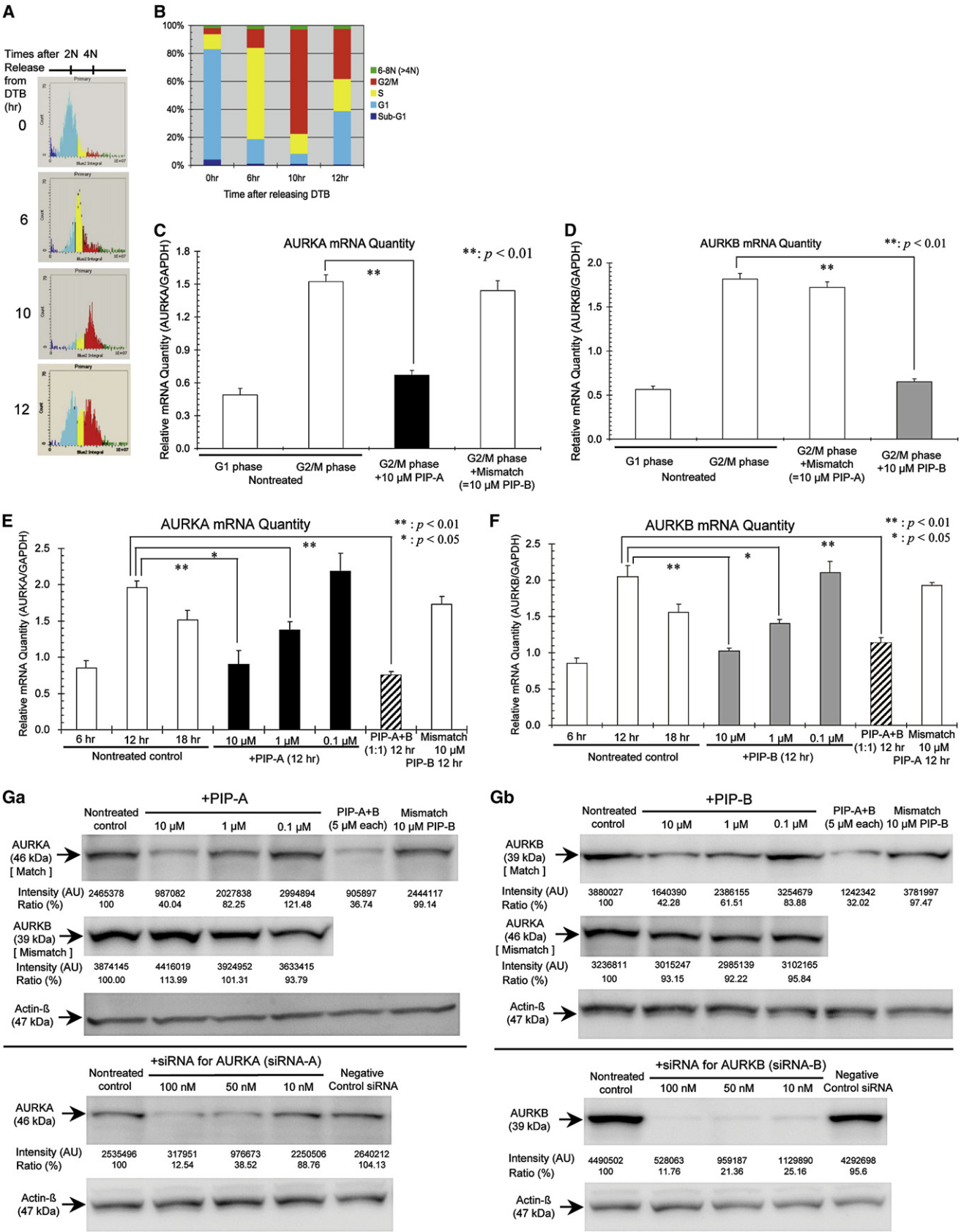
A
Times after Release from DTB (hr)
2N 4N
0
6
10
12
B
100%
80%
60%
40%
20%
0%
6-8N (>4N)
G2/M
S
G1
Sub-G1
0hr
6hr
10hr
12hr
Time after releasing DTB
C
AURKA mRNA Quantity
**: p < 0.01
Relative mRNA Quantity (AURKA/GAPDH)
G1 phase
G2/M phase
Nontreated
G2/M phase +10 μM PIP-A
G2/M phase +Mismatch (=10 μM PIP-B)
D
AURKB mRNA Quantity
**: p < 0.01
Relative mRNA Quantity (AURKB/GAPDH)
G1 phase
G2/M phase
Nontreated
G2/M phase +Mismatch (=10 μM PIP-A)
G2/M phase +10 μM PIP-B
E
AURKA mRNA Quantity
** : p < 0.01
* : p < 0.05
Relative mRNA Quantity (AURKA/GAPDH)
6 hr
12 hr
18 hr
Nontreated control
10 μM
1 μM
0.1 μM
+PIP-A (12 hr)
PIP-A+B (1:1) 12 hr
Mismatch 10 μM PIP-B 12 hr
F
AURKB mRNA Quantity
** : p < 0.01
* : p < 0.05
Relative mRNA Quantity (AURKB/GAPDH)
6 hr
12 hr
18 hr
Nontreated control
10 μM
1 μM
0.1 μM
+PIP-B (12 hr)
PIP-A+B (1:1) 12 hr
Mismatch 10 μM PIP-A 12 hr
Ga
+PIP-A
Nontreated control
10 μM
1 μM
0.1 μM
PIP-A+B (5 μM each)
Mismatch 10 μM PIP-B
AURKA (46 kDa) [Match]
Intensity (AU) 2465378 987082 2027838 2994894 905897 2444117
Ratio (%) 100 40.04 82.25 121.48 36.74 99.14
AURKB (39 kDa) [Mismatch]
Intensity (AU) 3874145 4416019 3924952 3633415
Ratio (%) 100.00 113.99 101.31 93.79
Actin-ß (47 kDa)
+siRNA for AURKA (siRNA-A)
Nontreated control
100 nM
50 nM
10 nM
Negative Control siRNA
AURKA (46 kDa)
Intensity (AU) 2535496 317951 976673 2250506 2640212
Ratio (%) 100 12.54 38.52 88.76 104.13
Actin-ß (47 kDa)
Gb
+PIP-B
Nontreated control
10 μM
1 μM
0.1 μM
PIP-A+B (5 μM each)
Mismatch 10 μM PIP-B
AURKB (39 kDa) [Match]
Intensity (AU) 3880027 1640390 2386155 3254679 1242342 3781997
Ratio (%) 100 42.28 61.51 83.88 32.02 97.47
AURKA (46 kDa) [Mismatch]
Intensity (AU) 3236811 3015247 2985139 3102165
Ratio (%) 100 93.15 92.22 95.84
Actin-ß (47 kDa)
+siRNA for AURKB (siRNA-B)
Nontreated control
100 nM
50 nM
10 nM
Negative Control siRNA
AURKB (39 kDa)
Intensity (AU) 4490502 528063 959187 1129890 4292698
Ratio (%) 100 11.76 21.36 25.16 95.6
Actin-ß (47 kDa)

2004; Meraldi et al., 2002; Ota et al., 2002; Sorrentino et al., 2005; Tanaka et al., 2002). The 1:1 combination treatment demonstrated various grades of anti-proliferative synergy in all of these human tumor cell lines, with IC_{50} values in the ~5–20 μM range (Table 2). These results revealed that the 1:1 combination treatment had a broad-spectrum antiproliferative synergy for human tumor cells. In contrast, the human normal cell lines, such as MRC5 and HUVECs, demonstrated potent resistance to the antiproliferative synergy of the 1:1 combination treatment (Figure 4D and Table 2). These data suggest that the 1:1 combination treatment may not affect human normal cells within the effective concentration range for human tumor cells.

Effect of PIP-A and PIP-B on Cell-Cycle Progression of Human Tumor Cells

The effects of PIP-A and PIP-B on cell-cycle progression were examined in random cultured HeLa cells by laser-scanning cytometry (iCys System™; CompuCyte Corp.) (Figure 5A). In the nontreated control cells (including 1% DMSO), the cell-cycle progression was almost completely conserved every 12 hr (Figure 5A, lane 1). However, the 1:1 combination treatment with PIP-A and PIP-B caused prominent confusion between 24 and 48 hr on the DNA content histograms (Figure 5A, lane 4). This interesting phenotype indicated the serious catastrophe of cell-cycle progression, such as failure of mitosis and cytokinesis. In addition, the prominent accumulation of cells with DNA contents less than 2N at sub-G1 phase and greater than 4N was observed during 36 to 48 hr (Figure 5A, lane 4). This abnormal cell accumulation indicated that the former was DNA fragmentation in apoptotic cells and the latter was DNA aneuploidy caused by mitotic arrest. Therefore, these results strongly suggested that the 1:1 combination treatment synergistically induced the serious catastrophe of cell-cycle progression mediated by mitotic arrest followed by tumor cell death (apoptosis). Although the dose is below both IC_{50} values, the single treatment with 10 μM of PIP-A or PIP-B had only a slight influence on the cell-cycle progression (Figure 5A, lanes 2 and 3).

Apoptosis Detection Assay Results

A consequence of the mitotic abnormality induced by the PIPs could be activation of the apoptotic pathway, particularly in the combination treatment of cells with PIP-A and PIP-B. To identify this possibility, HeLa cells treated with PIPs for 48 hr were stained by FITC-conjugated Annexin V and propidium iodide (PI) and were subjected to the fluorescence microscopic analysis (Figure 5B) and flow cytometric (FACScan®) analysis (Figure 5C). In addition, the effects of PIPs for human normal cell line were similarly examined using HUVECs by FACS analysis, as a reference experiment.

Most of the nontreated control cells (including 1% DMSO) were double negative for FITC-Annexin V and PI staining (Figure 5B, lane 1) and remained in the lower left (LL) quadrant of dot plots (92.96%) (Figure 5Cb), which indicates the viable cells. In contrast, a significant increase of the FITC-Annexin V-positive cells was demonstrated in the 1:1 combination treatment with PIP-A and PIP-B assessed at 48 hr (Figure 5B, lane 4), and the cells were in the lower right (LR) quadrant of dot plots (33.66%), which indicates the early apoptotic cells (Figure 5C). This FACS result is completely consistent with the apoptotic cell death in cells treated with 200 μM cisplatin as a positive control (Figure 5C). In addition, the prominent ladder DNA that revealed the apoptotic DNA fragmentation was detected in the 1:1 combination treatment (Figure 5D, lane 4). The cells treated with 10 μM of PIP-A were almost the same as the nontreated control cells (Figure 5B, lane 2 and Figure 5C). In single treatment with 10 μM of PIP-B, the slight increase of the early apoptotic cells was demonstrated in Figure 5B, lane 3 and Figure 5C. The reference experiment result (FACS analysis) was shown in Figure S3. In HUVECs, there was almost no effect against all of the treatment with PIPs for 48 hr (Figure S3).

DISCUSSION

Synthetic PIP has been reported to bind target sites within nucleosomes and may influence chromatin structure (Bando et al., 2002; Best et al., 2003; Dervan, 2001; Matsuda et al., 2006; Murty and Sugiyama, 2004; Nickols and Dervan, 2007; Nickols et al., 2007; Trauger et al., 1996; Zhang et al., 2006). Since PIPs can be readily designed and synthesized to target any sequence of biological interest, they may be useful in the investigations of gene function and perhaps in gene therapy (Bando et al., 2002; Best et al., 2003; Dervan, 2001; Matsuda et al., 2006; Murty and Sugiyama, 2004; Nickols and Dervan, 2007; Nickols et al., 2007; Trauger et al., 1996; Zhang et al., 2006). Inhibition of gene expression by PIPs that target regulatory sequences on promoter (5′-flanking) regions may be a biologically and physiologically relevant strategy because PIPs suppress the enhancing effect of transcription factors and preserve the baseline expression of the target gene. Therefore, the suppression or knockdown of enhanced target gene expression by PIPs may be more practical as novel antitumor agents since PIPs can efficiently inhibit only the overexpression of target gene in tumor cells without damaging the baseline expressions required for normal cells. Several recent investigations of PIPs have focused

Figure 3. Knockdown Effect of PIP-A and PIP-B

(A) DNA content histogram of HeLa cells released from DTB and analyzed by laser-scanning cytometry.

(B) Percentages of cells at each phase of the cell cycle in synchronized HeLa cell populations.

(C and D) Induction of AURKA and AURKB mRNA expression and knockdown effect of PIP-A and PIP-B during G2/M phase, measured by real-time quantitative PCR assay. The data are presented as the mean ± standard deviation (SD) of six independent experiments (n = 6). Tukey's multiple comparison test was used for statistical analysis.

(E and F) Knockdown effects of PIP-A and PIP-B for mRNA expression in random cultured cells. Relative AURKA and B mRNA quantities (AURKA or AURKB/GAPDH) were measured by real-time PCR assay. The data are presented as the mean ± standard deviation (SD) of six independent experiments (n = 6). Tukey's multiple comparison test was used for statistical analysis.

(G) WB analysis results (AURKA, AURKB, and Actin-β). Knockdown effects of PIP-A and PIP-B for protein levels in random cultured cells were measured by WB analysis. The intensity values of respective blotting bands were analyzed by the software Multi Gauge™ version 3.0 of attachment in LAS3000 (Fujifilm). AU, arbitrary unit. Actin-β is used as a loading control. As reference experiments, the siRNAs to repress each AURKA or AURKB (siRNA-A and siRNA-B) were used.

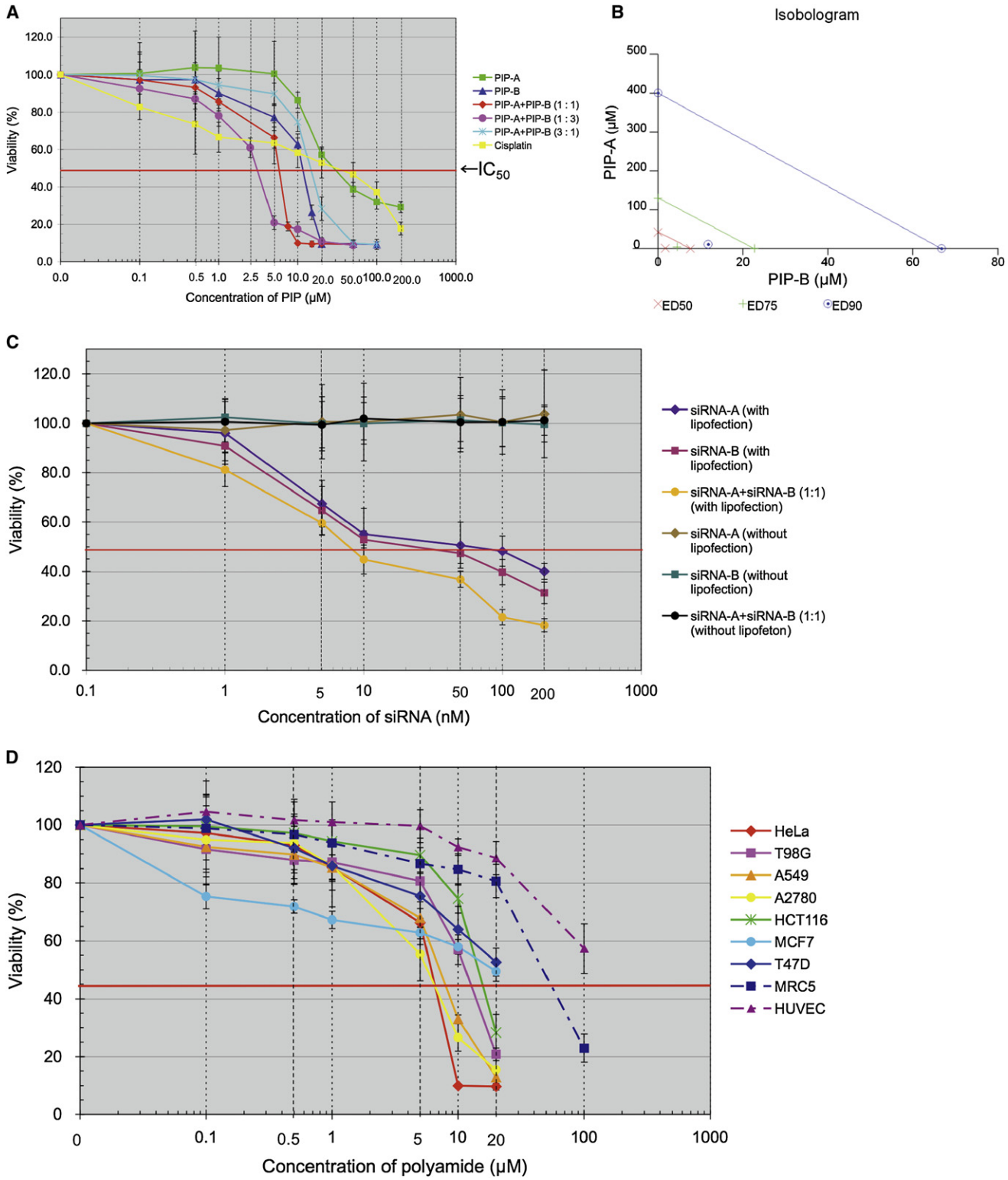

Figure 4. In Vitro Cell Viability Assay and Combination Assay Results

The cell viability assays were performed by the WST-8™ (Nacalai Tesque, Inc.) protocol. Red line represents the IC_{50}.

(A) Cell viability assay for HeLa cells treated with PIPs and cisplatin. The data are presented as the mean ± standard deviation (SD) of six independent experiments (n = 6).

(B) The isobologram at 1:1 combination treatment with PIP-A and PIP-B for ED 50, 75, and 90.

(C) Cell viability assay for HeLa cells transfected siRNAs with or without use of lipofection. The data are presented as the mean ± standard deviation (SD) of six independent experiments (n = 6).

Table 2. In Vitro Tumor Cell Growth Inhibiting Activity of PIP-A and PIP-B

	Cell Type	IC_{50} (μM)	CI (ED_{50})[a]
HeLa	Human cervical adenocarcinoma		
PIP-A		25.47	
PIP-B		11.76	
*PIP-A + PIP-B (1:1)		5.89	0.256
*PIP-A + PIP-B (3:1)		15.41	0.655
*PIP-A + PIP-B (1:3)		3.24	0.259
Cisplatin		33.92	
siRNA-A (with lipofection)		68.75 (nM)	
siRNA-B (with lipofection)		23.61 (nM)	
*siRNA-A + siRNA-B (with lipofection)		7.89 (nM)	0.525
*PIP-A + PIP-B (1:1)			
Human Tumor Cell Lines			
T98G	Glioblastoma	12.39	
A549	Non-small cell lung cancer	7.57	
A2780	Ovarian cancer	5.94	
HCT116	Colon cancer	15.31	
MCF7	Breast cancer	19.36	
T47D	Breast cancer	>20.00	
Human Normal Cell Lines			
MRC5	Lung fibroblast cell	62.46	
HUVECs	Umbilical vein endothelial cell	> 100.00	

[a] CI values at ED_{50} were calculated by CalcuSyn software (version 2.0) on the basis of the data of Figure 4A (ED_{50} = IC_{50}). CI > 1.0 indicates antagonism, CI = 1.0 indicates additivity, a d CI < 1.0 indicates synergism.

on the structural characterization of transcription factor-DNA complexes within promoter sequences (Matsuda et al., 2006; Nickols and Dervan, 2007; Nickols et al., 2007; Yang et al., 2007).

The Aurora/Ipl1p kinase family, in particular AURKA and AURKB, is a key regulator of mitosis and is essential for the accurate and equal segregation of genomic material from parent to daughter cells (Carvajal et al., 2006; Jung et al., 2006; Kimura et al., 2004; Tanaka et al., 2002). The levels of mRNA expression and protein of AURKA and AURKB are tightly regulated during the cell-cycle by the PRE, cell-cycle dependent element (CDE), and CHR on their respective promoters (Carvajal et al., 2006; Jung et al., 2006; Kimura et al., 2004; Tanaka et al., 2002). Dysregulation of Aurora kineses has been linked to tumorigenesis (Carvajal et al., 2006; Jung et al., 2006; Kimura et al., 2004; Tanaka et al., 2002). In this study, PIP-A and PIP-B were designed not to cover respective consensus sequences of PRE and CHR but to span their boundary with the intention of guaranteeing the specificity for AURKA and AURKB promoter sequences. Both PIPs demonstrated strong, fast, and specific binding to the respective target DNA in the EMSA and Biacore assays. Best et al. (2003) reported that various fluorescein-conjugated PIPs exhibit good nuclear uptake in a wide variety of cell lines. In our in vitro experiments, FITC-labeled PIP-A and PIP-B were distributed immediately and sufficiently in the nuclei of cultured cells without any delivery systems and were localized for long periods. Nucleic acid medicines, such as antisense DNA, ribozymes, siRNA, and decoys, have been developed as gene-silencing agents. Decoys, in particular, inhibit the binding of target transcription factors in a manner similar to that of PIPs. However, since these agents are degraded easily by nucleases, they require drug-delivery systems to distribute sufficiently for the target sequence in nuclei of living cells. Because PIPs are completely resistant to nucleases and can be permeated to nuclei from outer membrane without any delivery system, such as lipofection, PIPs may be more appropriate for gene-silencing agents.

Recently, the evidence linking Aurora overexpression and malignancy has stimulated biological interest in developing Aurora kinase inhibitors for cancer therapy (Carvajal et al., 2006; Ditchfield et al., 2003, 2005; Harrington et al., 2004; Hauf et al., 2003; Jung et al., 2006; Yang et al., 2007). Given their preclinical antitumor activity and potential for tumor selectivity, several small molecule inhibitors for Aurora kinase family (e.g., hesperadine [Hauf et al., 2003], ZM447439 [Ditchfield et al., 2003, 2005], MK0457 (previously VX-680) [Harrington et al., 2004], and AZD1152 [Yang et al., 2007]) have been developed and are undergoing evaluation in clinical trials. These small molecules directly affect kinase activity by occupying the ATP-binding pocket (Carvajal et al., 2006; Ditchfield et al., 2003, 2005; Harrington et al., 2004; Hauf et al., 2003; Jung et al., 2006; Yang et al., 2007) and act as broad and nonspecific inhibitors for Aurora kinases in a similar manner. ZM447439 inhibits AURKA and AURKB activities (Ditchfield et al., 2003, 2005), hesperadine reveals preferential inhibition for AURKB (Hauf et al., 2003), and MK0457 acts as a pan Aurora kinase inhibitor (Harrington et al., 2004). Therefore, each small molecule also induces a similar phenotype in cell-based assays, characterized by the inhibition of phosphorylation for histone H3 on Ser^{10}, cytokinesis, and the development of aneuploidy (Carvajal et al., 2006; Ditchfield et al., 2003, 2005; Harrington et al., 2004; Hauf et al., 2003; Jung et al., 2006; Yang et al., 2007). Interestingly, although ZM447439 and MK0457 inhibited both AURKA and AURKB activity and induced failure of cytokinesis and apoptosis in vitro, the phenotypes in treated cells with each agent were regarded as the result of inhibition for AURKB, not for AURKA (Ditchfield et al., 2003, 2005; Harrington et al., 2004). Since the antitumor activity of both ZM447439 and MK0457 was primarily due to AURKB inhibition, the specific AURKB inhibitor, such as AZD1152, have been developed (Yang et al., 2007).

In this study, PIP-A and PIP-B demonstrated significantly specific knockdown effects for mRNA expression and protein levels of AURKA and AURKB. These results indicate that both PIPs have potential use, predominantly as experimental tools in functional analysis of Aurora kinases and as gene-silencing therapeutic agents, depending on the specificity of PIP-A and PIP-B as the inhibitors. In addition, the combination treatment with PIP-A and PIP-B revealed potent antiproliferative synergy for human tumor cell lines in vitro. This biologically interesting phenotype indicates that, as a result of direct binding to each target gene sequence, both PIPs specifically and independently regulate AURKA and AURKB gene expression, respectively,

(D) Cell viability assay for several human tumor cell lines and normal cell lines treated with combination of PIP-A and PIP-B. The data are presented as the mean ± standard deviation (SD) of six independent experiments (n = 6).

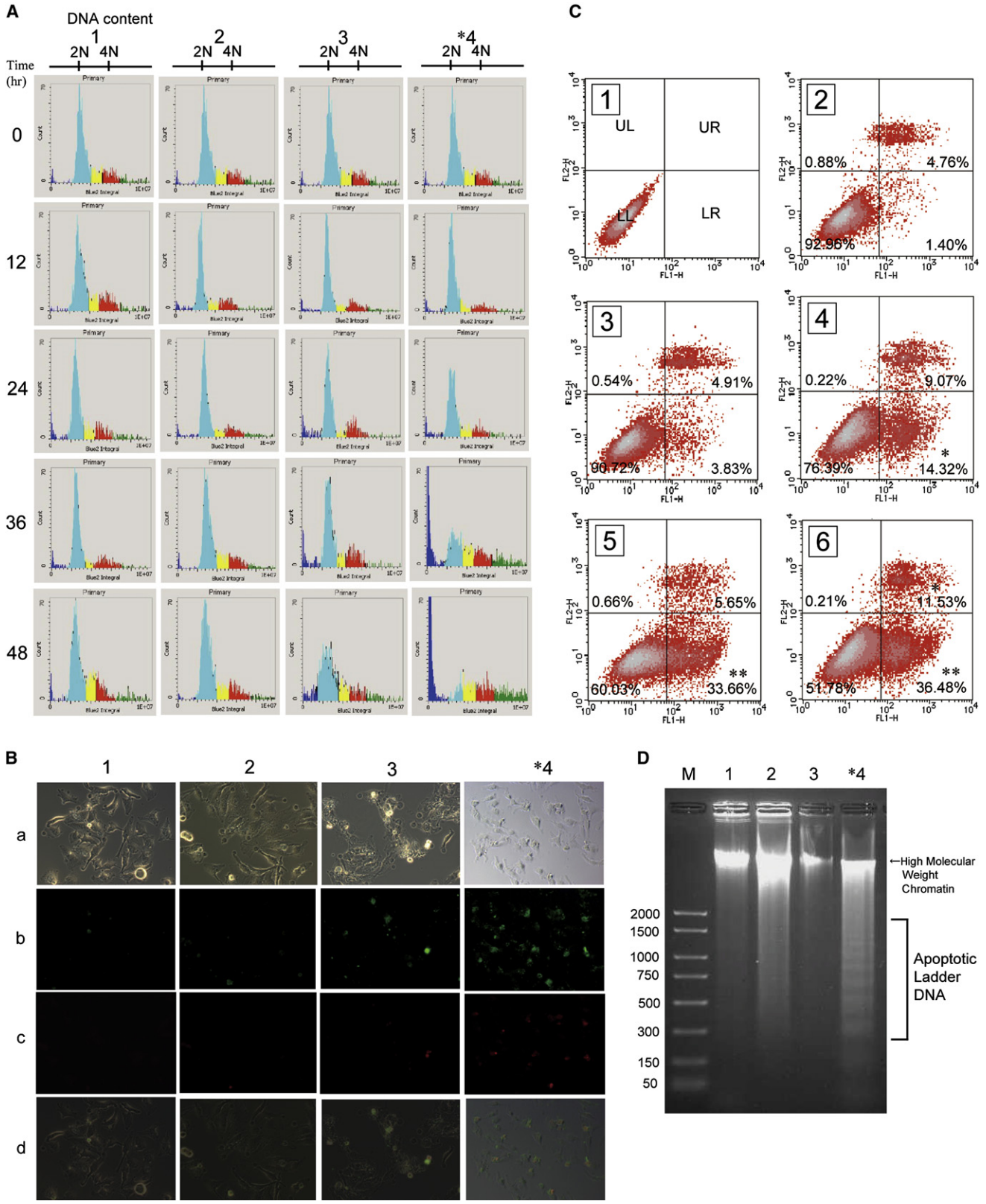

Figure 5. The Effect of PIP-A and PIP-B against Cell Cycle

(A) Cell-cycle progression analysis results. DNA content histogram of HeLa cells treated with respective PIPs in random cultured cell conditions, analyzed by Laser-scanning cytometry. Lane 1, nontreated control cells (including 1% DMSO); lane 2, PIP-A (10 μM); lane 3, PIP-B (10 μM); and lane 4, 1:1 PIP-A + PIP-B (5 μM each).

and cause prominent growth inhibition of tumor cells synergistically. The combination assay results indicate the PIP-B dominant antiproliferative synergy and are consistent with previous investigations using ZM447439 and MK0457 (Ditchfield et al., 2003, 2005; Harrington et al., 2004). In addition, these results suggest that the more practical antiproliferative synergy might be obtained by variously changing the combination rate of PIP-A and PIP-B. The effectiveness of combination treatment was also confirmed by the supporting reference experiments using siRNAs. This synergistic phenotype resulted from the catastrophe of cell-cycle progression due to the combination treatment with both PIPs. This result indicates that the combination treatment induces the development of aneuploidy caused by mitotic arrest, cellar growth inhibition, and apoptosis, consistent with the results of previous investigations (Carvajal et al., 2006; Ditchfield et al., 2003, 2005; Harrington et al., 2004; Hauf et al., 2003; Jung et al., 2006; Yang et al., 2007). However, each PIP specifically degraded the total protein level of AURKA or AURKB due to suppressing gene expression, without inhibition of the respective kinase activities. Therefore, the synergy of PIP-A and PIP-B appeared more gradually, compared with the effect of previously reported small molecule kinase inhibitors (Carvajal et al., 2006; Ditchfield et al., 2003, 2005; Harrington et al., 2004; Hauf et al., 2003; Jung et al., 2006; Yang et al., 2007). Moreover, IC_{50} values of combination treatment for various tumor cell lines were within the 3–20 μM range. Regrettably, these effective dose ranges were significantly higher than those of previously reported small molecule kinase inhibitors and siRNAs and were inconsistent with the binding (Biacore) assay results, with dissociation constants within nanomolar range. We speculate that one of the major reasons for these results is the mild KDE of PIPs for gene expression. The each KDE of 10 μM of PIP-A and PIP-B was ~50% in the real-time quantitative PCR assay and WB analysis. These results may suggest that the recognizable sites that both PIPs target (7 or 8 bp) are of insufficient length to provide high specificity in the in vitro assays using cellular systems, although the high and specific binding constants of PIPs for target sequences are confirmed in cell-free analysis systems, such as Biacore. If the binding ability of PIPs for target sequence is only dependent on the recognition for linear combination of Watson-Crick base pairs, the PIP that is designed to recognize 7 or 8 bp site needs to distinguish 13,000–50,000 different candidate sequences (Dervan, 2001). However, the candidate binding sites of PIP must be more limited actually since PIP selectively recognizes and binds to the open and intact sequences in the minor groove of double-helical DNA (Dervan, 2001). To solve this query, further studies based on the comprehensive analysis to investigate the global effects of PIP using gene chip assay (Nickols and Dervan, 2007) or the improvement of the structure of PIP as a chemical compound (Bando et al., 2002; Murty and Sugiyama, 2004; Zhang et al., 2006) may be needed.

Normal human cell lines were resistant to the antiproliferative synergy of the combination treatment with PIP-A and PIP-B. These results suggest that the combination treatment may have significantly selective toxicity for proliferating tumor cells in vitro. Both PIP-A and PIP-B are designed to target the cell-cycle-dependent positive regulatory (enhancing) regions on the respective AURKA and AURKB promoter sequences. Therefore, this selectivity may be based on inhibitory effects of both PIPs only for the cell-cycle-dependent overexpression of AURKA and AURKB in tumor cells, without damaging the baseline expression required for normal cells. However, in the present study, the unfavorable toxicity of both PIPs to rapidly dividing human normal cells in the hematopoietic and gastrointestinal systems was not examined; therefore, further investigation of the pharmacological safety of both PIPs is needed using in vivo toxicology animal studies.

SIGNIFICANCE

In conclusion, we developed novel small molecule PIPs targeting AURKA and AURKB promoters—PIP-A and PIP-B, respectively. Our observations indicated that PIP-A and PIP-B specifically inhibited both mRNA expression and protein levels of AURKA and AURKB as a result of binding to the active regions on the respective promoters. In addition, both PIPs revealed potent antiproliferative synergy to human tumor cell lines as a result of inducing apoptosis-mediated severe catastrophe of cell-cycle progression. These results suggest that PIP-A and PIP-B may be selectively toxic to proliferating tumor cells and, therefore, open up new opportunities to develop novel antitumor agents. To our knowledge, there has been no report such as this study, and further investigation and development concerning PIPs targeting AURKA and AURKB are expected.

EXPERIMENTAL PROCEDURES

This study was approved by the Nihon University Institutional Review Board.

Polyamide Synthesis: Machine-Assisted Solid-Phase Protocols

All PIP compounds were synthesized at Gentier Biosystems, Inc. (Kyoto, Japan). PIP-A and PIP-B were purchased from Gentier Biosystems, Inc. Both PIPs were synthesized according to previously established methods (Bando et al., 2002; Murty and Sugiyama, 2004; Zhang et al., 2006). The synthesis protocol of PIP is briefly described as follows.

All machine-assisted PIP syntheses were performed on a Pioneer Peptide Synthesizer (Applied Biosystems) with a computer-assisted operation system at a 0.10 mmol scale (100 mg of wang resin, 0.96 mequiv/g) by using Fmoc chemistry. The following conditions were used in all PIP solid-phase syntheses for each cycle: deblocking for 5 min with 20% piperidine/DMF, activating for 2 min with 0.5 M HCTU/DMF and 1.0 M DIEA/ DMF, coupling for 60 min, and capping for 5 min with 5% acetic anhydride/5% pyridine/DMF. After the completion of the synthesis, the resin was washed with a mixture of methanol/DCM

(B) Apoptosis detection assay-1: Fluorescence microscopic analysis results. Lane 1, nontreated control cells (including 1% DMSO); lane 2, PIP-A (10 μM); lane 3, PIP-B (10 μM); and lane 4, 1:1 PIP-A + PIP-B (5 μM each). (a) Bright field, (b) Annexin V FITC, (c) propidium iodide (PI), and (d) merge.
(C) Apoptosis detection assay-2: Flow cytometric analysis results. *x* axis,: Annexin V-FITC fluorescence (log scale); and *y* axis, PI fluorescence (log scale). Total analysis cell counts, 40000. LL (lower left), viable cells; LR (lower right), early stage of Apoptosis; UR (upper right), progressive (late) stage of apoptosis or necrosis. C-1, nonlabeled control (Annexin V-FITC and PI double negative); C-2, nontreated control cells (including 1% DMSO); C-3, PIP-A (10 μM); C-4, PIP-B (10 μM); C-5, (1:1) PIP-A + PIP-B (5 μM each); and C-6, positive control treated with 200 μM cisplatin.
(D) Apoptosis detection assay result. −3, DNA fragmentation detection assay results. Lane 1, nontreated control cells (including 1% DMSO); lane 2, PIP-A (10 μM); lane 3, PIP-B (10 μM); a d lane 4, 1:1 PIP-A + PIP-B (5 μM each).

(1/1, v/v) (3 ml) and was dried by vacuum desiccation. The resin was then placed in a 20 ml glass scintillation vial, 5 ml of dimethylamino propylamine was added, and the solution was stirred at 55°C overnight. Resin was removed by filtration through a pad of Celite and was washed thoroughly with methanol/DCM (1/1, v/v). The residue was dissolved in approximately 0.5 ml of DMF. The resulting PIP solution was analyzed and purified by analytical HPLC as follows; Chemcobond 5-ODS-H reversed phase column (150 × 20 mm) in 0.1% AcOH with acetonitrile as eluent at a flow rate of 9.9 ml/min appropriate gradient elution conditions, and detection at 254 or 370 nm. After confirmation by ESI-Mass, appropriate fractions were lyophilized to give the final desired polyamides as white powders.

DNA-Binding Assay

For the EMSA, FITC-labeled match 22 bp oligo corresponding to AURKA and AURKB promoters including respective PIP-A and PIP-B binding sites were synthesized (Table S1). In addition, the mismatch-1 22 bp oligo, including 2 bp mutations within respective PIP-A and PIP-B binding sites, were prepared (Table S1). The appropriate sense and antisense oligo-DNA were annealed for preparing double strand (ds)-oligo. The binding reaction was performed at 37°C for 1 hr in 20 μl binding buffer containing 10 μM ds-oligo and 50 μM PIP. Gel electrophoresis was performed on a 20% polyacrylamide gel at 300V for 3–4 hr at 4°C. The EMSA results were visualized by luminescent image analyzer LAS3000 (Fujifilm).

The kinetics for binding of PIP to the target sequence were evaluated by the surface plasmon resonance technique with a molecular interaction model. Biotin-labeled match oligo corresponding to AURKA and AURKB promoters and mismatch oligo including 2 bp mutations were synthesized (Table S1). Biotin-labeled oligos were annealed for double strand and were immobilized (1 μM) on a streptavidin-functionalized sensor chip SA (Biacore). The kinetics of interaction between PIP and biotin-labeled ds-oligo were measured using Biacore 2000 system (Biacore). The data of binding responses were fitted to Langmuir double molecular interaction model with mass transport.

Distribution of FITC-Labeled PIP In Vitro

HeLa cells were seeded on 6-well plates, to 3.0 × 10^4 cells per well, and were grown in 2 ml of Dulbeco's modified Eagle's medium (DMEM) (Sigma) with 10% fetal calf serum (FCS) (Sigma) and antibiotics. Cells were maintained at 37°C in 5% CO_2. After 24 hr, HeLa cells were incubated with final 10 μM of FITC-labeled PIP in growth medium for 6, 12, 24, and 48 hr, respectively. After incubation with FITC-labeled PIP, cells were viewed at 200× magnification under live cell conditions. Afterward, cells were washed with phosphate-buffered saline (PBS) and fixed in 4% paraformaldehyde for 10 min. Nuclei were stained by Hoechst 33342 (Invitrogen) for 30 min and then were viewed again.

Construction of Promoter Plasmid for AURKA and AURKB

To obtain 5′-flanking regions of AURKA and AURKB gene, human genomic DNA was extracted from human blood cells using the conventional phenol-chloroform method and ethanol precipitation. Using this human genomic DNA as a template, 1.8 and 2.4 kb of the 5′-flanking regions of AURKA and AURKB gene (including the first exon) were amplified using a standard PCR technique. Two pairs of primers that were specific for AURKA and AURKB promoters were prepared (Table S1). The restriction enzyme linker was incorporated into the 5′ end of each primer (Table S1). Both gel-purified PCR products were digested at both ends by restriction enzymes and then were cloned into the pGL3-basic firefly luciferase-reporter plasmid (Promega). The sequence of each DNA fragment inserted into the pGL3-basic vector was confirmed by direct sequencing in both strands.

Dual-Luciferase Reporter Assay

HeLa cells were seeded on 24-well plates and grown until preconfluence in DMEM with 10% FCS. The pGL3-basic reporter plasmid, including AURKA or AURKB promoter, was transiently cotransfected into HeLa calls together with phRG-TK vector (Promega) using Lipofectamine™ 2000 (Invitrogen) as described previously (Jung et al., 2006; Matsuda et al., 2006; Tanaka et al., 2002). Firefly luciferase activity values of each reporter plasmid were normalized by Renilla luciferase activity values expressed from phRG-TK vector as the internal control, to allow for variation in transfection efficiency. Luciferase activity was measured using a Wallac 1420 multilabel counter (Amersham Bioscience).

Cell-Cycle Synchronization Analysis

HeLa cells were seeded on 6-well plates to 3.0 × 10^4 cells per well and were synchronized at the G1/S boundary by a DTB protocol as previously described (Tanaka et al., 2002). The DNA content of cells was analyzed by laser-scanning cytometry (iCys System™; CompuCyte Corp.) during the time course after release from DTB.

Real-Time Quantitative PCR Assay

Total RNA was extracted from the collected appropriate HeLa cell lysates, using an RNeasy-Mini Kit (QIAGEN Science), and then was reverse-transcribed using a PrimeScript™ RT reagent Kit (TaKaRa Bio Inc.) according to the manufacturer's instructions. AURKA and AURKB mRNA expression were analyzed by real-time quantitative PCR assay (Thermal Cycler Dice® Real Time System; TaKaRa Bio Inc.) using SYBR Premix Ex *Taq* (TaKaRa Bio Inc.). The expression level of GAPDH gene was used as the internal control to normalize for differences in input cDNA. Assay-on-Demand primers for AURKA (HA038310), AURKB (HA089596), and GAPDH (HA067812), which were set from exons separated by introns, were purchased from TaKaRa Bio Inc. (Table S1).

Western Blot Analysis

Preconfluent HeLa cells were cultured with 10% FCS medium and were untreated or exposed to various concentrations of PIPs for 12 hr. Lysates were clarified by centrifugation at 1500 rpm for 3 min with PBS, the signaling of the cells was stopped by adding SDS-sample buffer, and the extracts were loaded to SDS-PAGE and transferred a polyvinylidene difluoride membrane (Millipore, Bedford, MA). After transfer, the blots were incubated with blocking solution (5% skim milk) in washing buffer (20 mM Tris-HCl [pH 7.4], 8% NaCl, and 0.0005% Tween-20) and were probed with primary antibodies diluted in the blocking solution, respectively. Total AURKA, AURKB, and Actin-β were detected with anti-AURKA, AURKB, and Actin-β antibody (abcam). These signals were identified using HRP-conjugated secondary antibodies and enhanced chemiluminescent substrate (Millipore, Bedford, MA), according to the manufacturer's instructions, and were visualized by a luminescent image analyzer LAS3000 (Fujifilm).

RNAi Technique

Stealth™ siRNA duplexes (Invitrogen) designed to repress AURKA and AURKB (siRNA-A and siRNA-B; Table S1) were transfected using Lipofectamine™ 2000 (Invitrogen) according to the manufacturer's instructions.

In Vitro Cell Viability Assay and Combination Effect Analysis

All cell lines were seeded on a 96-well microplate to 3.0 × 10^3 cells per well and cultured in DMEM with 10% FCS at 37°C in 5% CO_2. The tested PIPs were dissolved in growth medium at appropriate concentrations and were treated for 48 hr. In addition, cisplatin was purchased from Sigma. The nontreated control cells were cultured in media containing 1% DMSO. Resulting metabolically active cells were evaluated by the subsequence color reaction. The cell viability assays were performed using the WST-8™ (Nacalai Tesque, Inc.) protocol. The absorbance (A_{450}) of each well was measured using a Wallac 1420 multilabel counter (Amersham Bioscience).

The CI values at ED_{50} were calculated by the previously established Median-effect algorithm (Chou and Talalay, 1984; Damaraju et al., 2007) using CalcuSyn software (version 2.0; Biosoft) based on the data of in vitro cell viability assay ($ED_{50} = IC_{50}$). CI > 1.0 indicates antagonism, CI = 1.0 indicates additivity, and CI < 1.0 indicates synergism.

Cell-Cycle Progression Analysis

HeLa cells were seeded on 6-well plates to 3.0 × 10^4 cells per well and were cultured with 10% FCS medium. After incubation for 6 hr, the medium was switched to the new one containing final 10 μM of PIP. This time point was designated "time 0." After 12, 24, 36, and 48 hr of incubation, the monolayer cells were washed with PBS and fixed in 4% paraformaldehyde for 10 min. Nuclei were stained by Hoechst 33342 (Invitrogen) for 30 min, and then the DNA content of cells was analyzed by laser-scanning cytometry (iCys system™). In general, more than 1.0 × 10^3 cells were examined in each well. Each phase of the cell-cycle was determined on the basis of the DNA contents.

Apoptosis Detection Assay

The apoptosis detection assay was performed using an Annexin V FITC Apoptosis Detection Kit (Calbiochem), according to the manufacturer's instructions. In brief, preconfluent (~5.0×10^5–1.0×10^6) HeLa cells were cultured with 10% FCS medium and treated with 10 μM of PIP for 48 hr. The cells were washed with PBS, stained with FITC-conjugated Annexin V and propidium iodide (PI), and then were subjected to the fluorescence microscopy analysis or the Becton Dickinson (BD) flow cytometric (FACScan®) analysis. In FACS analysis, 4.0×10^4 cells were examined in each sample. In addition, apoptotic DNA fragmentation was detected using a Suicide Track™ DNA Ladder Isolation Kit (Calbiochem), according to the manufacturer's instructions.

Statistical analysis

The statistical analysis, such as ANOVA and Tukey's multiple comparison test, was calculated using data analysis software program SPSS 13.0 for Windows. A value of $p < 0.05$ was considered statistically significant.

ACCESSION NUMBERS

The sequence for the gene encoding AURKA is available from the DDBJ/EMBL/GenBank™ database under accession number AL121914. The sequence for the gene encoding AURKB is also available from the DDBJ/EMBL/GenBank™ database under accession number AC135178.

SUPPLEMENTAL DATA

Supplemental Data include one table and three figures and are available online at http://www.chembiol.com/cgi/content/full/15/8/829/DC1/.

ACKNOWLEDGMENTS

This work was supported by "Academic Frontier" Project for Private Universities matching fund subsidy from the Ministry of Education, Culture, Sports, Science and Technology (grant 2006-2010).

Received: December 16, 2007
Revised: May 26, 2008
Accepted: June 6, 2008
Published: August 22, 2008

REFERENCES

Bando, T., Narita, A., Saito, I., and Sugiyama, H. (2002). Molecular design of a pyrrole-imidazole hairpin polyamides for effective DNA alkylation. Chemistry *8*, 4781–4790.

Best, T.P., Edelson, B.S., Nickols, N.G., and Dervan, P.B. (2003). Nuclear localization of pyrrole-imidazole polyamide-fluorescein conjugates in cell culture. Proc. Natl. Acad. Sci. USA *14*, 12063–12068.

Bischoff, J.R., Anderson, L., Zhu, Y., Mossie, K., Ng, L., Souza, B., Schryver, B., Flanagan, P., Clairvoyant, F., Ginther, C., et al. (1998). A homologue of *Drosophila aurora* kinase is oncogenic and amplified in human colorectal cancers. EMBO J. *17*, 3052–3065.

Carvajal, R.D., Tse, A., and Schwartz, G.K. (2006). Aurora kinases: new targets for cancer therapy. Clin. Cancer Res. *12*, 6869–6875.

Chou, T.C., and Talalay, P. (1984). Quantitative analysis of dose-effect relationships: the combined effects of multiple drugs or enzyme inhibitors. Adv. Enzyme Regul. *22*, 27–55.

Damaraju, V.L., Bouffard, D.Y., Wong, C.K., Clarke, M.L., Mackey, J.R., Leblond, L., Cass, C.E., Grey, M., and Gourdeau, H. (2007). Synergistic activity of troxacitabine (Troxatyl) and gemcitabine in pancreatic cancer. BMC Cancer *7*, 121–131.

Dervan, P.B. (2001). Molecular recognition of DNA by small molecules. Bioorg. Med. Chem. *9*, 2215–2235.

Ditchfield, C., Johnson, V.L., Tighe, A., Ellston, R., Haworth, C., Johnson, T., Mortlock, A., Keen, N., and Taylor, S.S. (2003). Aurora B couples chromosome alignment with anaphase by targeting BubR1, Mad2, and Cenp-E to kinetochores. J. Cell Biol. *161*, 267–280.

Ditchfield, C., Keen, N., and Taylor, S.S. (2005). The Ipl1/Aurora kinase family: methods of inhibition and functional analysis in mammalian cells. Methods Mol. Biol. *296*, 371–381.

Harrington, E.A., Bebbington, D., Moore, J., Rasmussen, R.K., Ajose-Adeogun, A.O., Nakayama, T., Graham, J.A., Demur, C., Hercend, T., Diu-Hercend, A., et al. (2004). VX-680, a potent and selective small-molecule inhibitor of the Aurora kinases, suppresses tumor growth in vivo. Nat. Med. *10*, 262–267.

Hauf, S., Cole, R.W., LaTerra, S., Zimmer, C., Schnapp, G., Walter, R., Heckel, A., van Meel, J., Rieder, C.L., and Peters, J.M. (2003). The small molecule Hesperadin reveals a role for Aurora B in correcting kinetochore-microtubule attachment and in maintaining the spindle assembly checkpoint. J. Cell Biol. *161*, 281–294.

Jung, F.H., Pasquet, G., Lambert-van der Brempt, C., Lohmann, J.J., Warin, N., Renaud, F., Germain, H., De Savi, C., Roberts, N., Johnson, T., et al. (2006). Discovery of novel and potent thiazoloquinazolines as selective Aurora A and B kinase inhibitors. J. Med. Chem. *49*, 955–970.

Kanda, A., Kawai, H., Suto, S., Kitajima, S., Sato, S., Takata, T., and Tatsuka, M. (2005). Aurora-B/AIM-1 kinase activity is involved in Ras-mediated cell transformation. Oncogene *24*, 7266–7272.

Kimura, M., Uchida, C., Takano, Y., Kitagawa, M., and Okano, Y. (2004). Cell cycle-dependent regulation of the human aurora B promoter. Biochem. Biophys. Res. Commun. *316*, 930–936.

Matsuda, H., Fukuda, N., Ueno, T., Tahira, Y., Ayame, H., Zhang, W., Bando, T., Sugiyama, H., Saito, S., Matsumoto, K., et al. (2006). Development of gene silencing pyrrole-imidazole polyamide targeting the TGF-β1 promoter for treatment of progressive renal diseases. J. Am. Soc. Nephrol. *17*, 422–432.

Meraldi, P., Honda, R., and Nigg, E.A. (2002). Aurora-A overexpression reveals tetraploidization as a major route to centrosome amplification in p53−/− cells. EMBO J. *21*, 483–492.

Murty, M.S., and Sugiyama, H. (2004). Biology of N-methylpyrrole- N-methylimidazole hairpin polyamide. Biol. Pharm. Bull. *27*, 468–474.

Nickols, N.G., and Dervan, P.B. (2007). Suppression of androgen receptor-mediated gene expression by a sequence-specific DNA-binding polyamide. Proc. Natl. Acad. Sci. USA *104*, 10418–10423.

Nickols, N.G., Jacobs, C.S., Farkas, M.E., and Dervan, P.B. (2007). Improved nuclear localization of DNA-binding polyamides. Nucleic Acids Res. *35*, 363–370.

Ota, T., Suto, S., Katayama, H., Han, Z.B., Suzuki, F., Maeda, M., Tanino, M., Terada, Y., and Tatsuka, M. (2002). Increased mitotic phosphorylation of histone H3 attributable to AIM-1/Aurora-B overexpression contributes to chromosome number instability. Cancer Res. *62*, 5168–5177.

Sorrentino, R., Libertini, S., Pallante, P.L., Troncone, G., Palombini, L., Bavetsias, V., Spalletti-Cernia, D., Laccetti, P., Linardopoulos, S., Chieffi, P., et al. (2005). Aurora B overexpression associates with the thyroid carcinoma undifferentiated phenotype and is required for thyroid carcinoma cell proliferation. J. Clin. Endocrinol. Metab. *90*, 928–935.

Tanaka, M., Ueda, A., Kanamori, H., Ideguchi, H., Yang, J., Kitajima, S., and Ishigatsubo, Y. (2002). Cell-cycle-dependent regulation of human aurora A transcription is mediated by periodic repression of E4TF1. J. Biol. Chem. *277*, 10719–10726.

Trauger, J.W., Baird, E.E., and Dervan, P.B. (1996). Recognition of DNA by designed ligands at subnanomolar concentrations. Nature *382*, 559–561.

Yang, J., Ikezoe, T., Nishioka, C., Tasaka, T., Taniguchi, A., Kuwayama, Y., Komatsu, N., Bandobashi, K., Togitani, K., Koeffler, H.P., et al. (2007). AZD1152, a novel and selective aurora B kinase inhibitor, induces growth arrest, apoptosis, and sensitization for tubulin depolymerizing agent or topoisomerase II inhibitor in human acute leukemia cells in vitro and in vivo. Blood *110*, 2034–2040.

Zhang, W., Bando, T., and Sugiyama, H. (2006). Discrimination of hairpin polyamides with an alpha-substituted-gamma-aminobutyric acid as a 5′-TG-3′ reader in DNA minor groove. J. Am. Chem. Soc. *128*, 8766–8776.

